

Equations of State for Ablator Materials in Inertial Confinement Fusion Simulations

P A Sterne, L X Benedict, S Hamel, A A Correa, J L Milovich, M M Marinak, P M Celliers and D E Fratanduono

Lawrence Livermore National Laboratory, Livermore, CA 94550, USA
Email: sterne1@llnl.gov

Abstract. We discuss the development of the tabular equation of state (EOS) models for ablator materials in current use at Lawrence Livermore National Laboratory in simulations of inertial confinement fusion (ICF) experiments at the National Ignition Facility. We illustrate the methods with a review of current models for ablator materials and discuss some of the challenges in performing hydrocode simulations with high-fidelity multiphase models. We stress the importance of experimental data, as well as the utility of ab initio electronic structure calculations, in regions where data is not currently available. We illustrate why Hugoniot data alone is not sufficient to constrain the EOS models. These cases illustrate the importance of experimental EOS data in multi-megabar regimes, and the vital role they play in the development and validation of EOS models for ICF simulations.

1. Introduction

The equation of state (EOS) of the ablator material controls many aspects of inertial confinement fusion (ICF) performance. The EOS strongly affects the ablation front pressure and temperature, controls the development of shocks at the ablation front, and determines the timing as the initial and subsequent shocks and release waves propagate through the ablator material. The EOS also controls the impedance match at the ablator-fuel interface [1], and so affects energy transfer via hydrodynamic processes into the fuel. Inertial Confinement Fusion (ICF) simulations at Lawrence Livermore National Laboratory (LLNL) use tabular EOS models to describe the EOS properties of the ablators and fuel. In this paper, we briefly describe some of the approaches used to construct these EOS models and highlight some ongoing work on selected ablator materials.

2. EOS Construction

Two different approaches are used to construct tabular EOS models for ICF ablators. The first is an extended version of the QEOS method [2] in which a global EOS is constructed using a simplified match between the solid and liquid phases that neglects latent heats. These models extend to high temperatures using the Purgatorio atom-in-jellium model [3] for the electron-thermal contributions. This includes atomic shell structure effects, which tends to give a better overall description of the ablation properties and resultant shock timings than the previously-used Thomas-Fermi approach.

The second approach uses an explicit multiphase EOS construction method. This is more complicated and time consuming than the simpler QEOS-based approach, since the resulting EOS depends sensitively on free-energy minimization across several phases. This approach, which is capable of capturing the complicated two-phase structure and latent heats of transition between solid



and liquid phases, has been used for the high-density carbon (HDC) EOS [4]. We will discuss some of the challenges in using these high-fidelity EOS models in hydrocode simulations.

EOS models are constructed by fitting experimental and theoretical data using physics-based models that extend over wide ranges of density and temperature. The EOS is constructed to fit the experimental data where available; ab initio calculations using quantum molecular dynamics (QMD) and path-integral Monte Carlo (PIMC) methods [5] are also used in the absence of experimental data.

3. Glow Discharge Polymer (GDP)

GDP is a carbon-hydrogen polymer with an approximate composition $\text{CH}_{1.36}$ [6]. The recommended EOS model, leos 5400, is constructed to fit a variety of data, most notably Hugoniot data [6], and “keyhole” data that measures the shock velocity change at the GDP-deuterium interface [1,7]. The Hugoniot data can be fit non-uniquely in a variety of ways, since trade-offs can be made between cold curve variations and thermal contributions, such as the anharmonic Grueneisen gamma term. The keyhole data provides a constraint on the off-Hugoniot behavior of the material, which narrows the possible trade-off choices and so constrains the EOS. Figure 1 shows the measured shock velocities in GDP and the resulting shock in deuterium, using leos 1014 for the deuterium EOS [8]. The two GDP EOS models 5310 and 5400 have similar Hugoniots (not shown), but the resulting deuterium shock velocities are very different, due to their differing off-Hugoniot behavior. This illustrates the importance of including data in addition to the Hugoniot data when constructing EOS models.

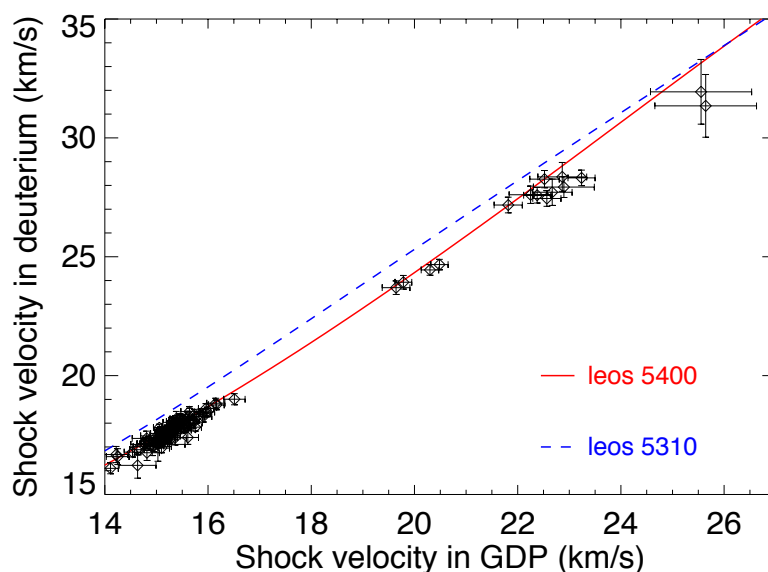


Figure 1. Measured shock velocities in GDP and resulting shock velocity in deuterium. Crosses are experimental data with error bars [9]. Lines are calculated using EOS models leos 5400 and 5310.

4. Beryllium

The currently recommended model for beryllium is XEOS 40. This is a QEOS model using Purgatorio-based electron-thermal contributions at high temperature. A multiphase model was also developed [10]; it is similar to XEOS 40, over much of its range, but has a more approximate extension to the Purgatorio-based higher temperature limit. The solid-solid phase transitions in Be do not appear to have a large effect on the EOS, so the benefit of the multiphase approach appears limited in this case, which justifies our current recommendation of the QEOS-based model.

In order to assess the accuracy of this EOS, we performed QMD simulations covering the Hugoniot pressure range from 3 to 7 Mbar using the VASP code [11]. We also estimated systematic uncertainties by performing calculations at one density with both local density and generalized-gradient [12] exchange-correlation functionals, and by comparing 2- and 4-electron pseudopotentials. The differences between these different approximations were small, and on the same order as the

difference between XEOS 40 and QMD results [13]. This suggests that the current EOS agrees fairly well with QMD simulations, but a slight adjustment may be needed. Future EOS modifications are planned, pending upcoming Hugoniot measurements in this pressure range on the Sandia Z machine.

5. Boron Carbide

Recent measurements on boron carbide provided Hugoniot data in the previously-unmeasured 3-8 Mbar region [14]. A new EOS model, leos 2121 was constructed to fit this data. In addition to Hugoniot data, the experimental data was analyzed to extract Eulerian sound speeds [15], which was found to disagree with the new EOS model. By simultaneously adjusting the cold curve and the Grueneisen gamma model, a new EOS model, leos 2122, was constructed to fit both sets of data, as shown in Fig. 2. This is another example of how it is not sufficient to constrain the EOS model with Hugoniot data alone. Additional data, in the form of sound speeds or release data, can help to resolve ambiguities in the decomposition of the EOS into cold and thermal terms.

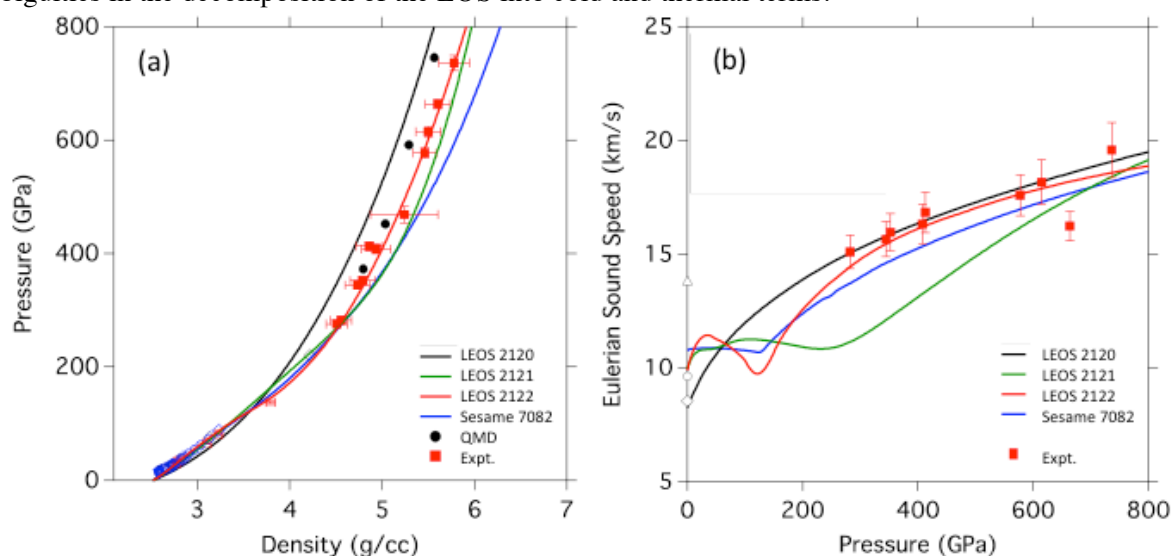


Figure 2. (a) Hugoniot for boron carbide EOS models compared with experiment. (b) Comparison of EOS models with Eulerian sound speed measurements along the Hugoniot. Experimental data is from Ref. [14].

6. High Density Carbon (HDC)

The recommended HDC EOS model is leos 9061. This is a multiphase EOS constructed on the basis of a comprehensive set of QMD and PIMC data and described in detail in Ref. [4]. Here, we focus on some of the resulting challenges for hydrocodes in using such high-fidelity EOS models with detailed latent heats and complicated melt curves.

HDC has the unusual property that its melt curve decreases with increasing density in the region where the Hugoniot crosses the melt curve. The EOS in this region features two solid phases and the melt phase, which results in a complicated set of isotherms for the ion-thermal energy, shown in Fig. 3. In hydrocodes, the derivatives of the energy with respect to temperature and density are used to estimate the change in density and temperature for a zone during a time-step. For this EOS, the derivatives near the melt region vary strongly with both density and temperature, which can result in anomalously large projected density or temperature updates. These, in turn, cause apparent noise in the calculations due to the creation of spurious shocks and releases caused by these unphysical density/temperature updates. In order to mitigate this effect in 1D implosions in the Hydra [16] code, it was necessary to place upper limits on the allowed changes in density and temperature at each time step. In subsequent work, changes have also been made to iterate on the projected update so that the change is not solely dependent on the prediction from the initial derivatives, but is corrected by the actual EOS at the proposed density-temperature value. These steps greatly reduced the noise in 1D simulations. Work is ongoing to address similar features in 2D simulations.

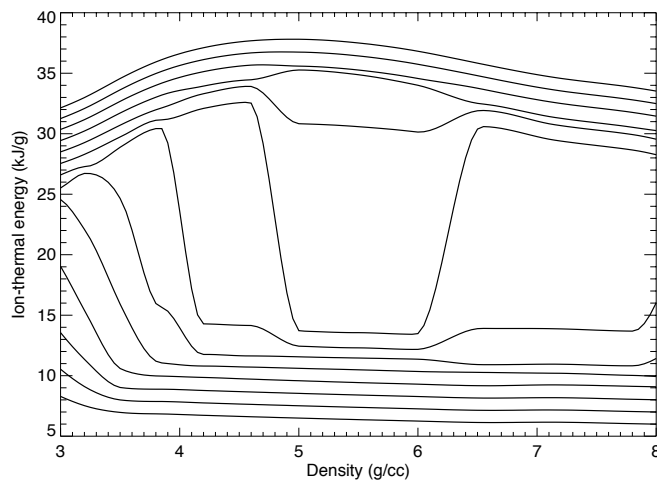


Figure 3. Ion-thermal energy isotherms for leos 9061 from 4000 K to 10000 K in 500 K steps.

7. Conclusions

The examples presented here have illustrated some of the challenges in constructing and using tabular EOS models, and some of the approaches that have been used to address these challenges. We stressed the importance of using electron-thermal models such as the Purgatorio model that includes shell-structure effects in order to produce accurate ablation-front behavior. We illustrated the importance of experimental data in the relevant density-temperature region, both Hugoniot data and additional data in form of sound-speed or release data at material interfaces, in order to resolve ambiguities between cold-curve and thermal EOS contributions. We indicated how ab initio QMD calculations can complement experimental data. We illustrated some of the problems in representing the physics associated with phase transitions in hydrocodes, and our initial steps to resolve these problems. The equation of state remains an important component in modeling ICF implosions, and improvements in EOS models based on additional experimental data and better theoretical models will lead to more accurate EOS representations and improved hydrodynamic modeling in ICF simulations.

8. Acknowledgments

This work was performed under the auspices of the U.S. Department of Energy by Lawrence Livermore National Laboratory under contract DE-AC52-07NA27344.

References

- [1] Robey H F et al 2012 *Physics of Plasmas* **19** 042706
- [2] More R M et al 1988 *Phys. Fluids* **31** 3059
- [3] Wilson B et al 2006 *Journal of Quantitative Spectroscopy and Radiative Transfer* **99** 658
- [4] Benedict L X et al 2014 *Phys. Rev. B* **89** 224109
- [5] Pollock E L and Ceperley D M 1984 *Phys. Rev. B* **30** 2555
- [6] Barrios M A et al 2012 *J. Appl. Phys.* **111** 093515
- [7] Hamel S et al 2012 *Phys. Rev. B* **86** 094113
- [8] Kerley G I 2003 *Sandia National Laboratories Report* SAND2003-3613
- [9] This set of 94 data points is an update of subsets that were previously published in Refs. [1,7]
- [10] Benedict L X et al 2009 *Phys. Rev. B* **79** 064106
- [11] Kresse G and Furthmüller J 1996 *Phys. Rev. B* **54** 11169
- [12] Perdew J P et al 1996 *Phys. Rev. Lett.* **77** 3865
- [13] Sterne P A and Hamel S 2015 unpublished
- [14] Fratanduono D E et al, in preparation
- [15] Fratanduono D E et al 2014 *J. Appl. Phys.* **116** 033517
- [16] Marinak M M et al 2001 *Physics of Plasmas* **8** 2275